

JGR Solid Earth

RESEARCH ARTICLE

10.1029/2018JB016453

Key Points:

- Recent marine surveys have identified over 1700 methane bubble plumes issuing from the northern Cascadia margin off Washington State
- Majority of the emission sites are grouped into a narrow band located near the western edge of the continental shelf and uppermost margin
- Multiple models for the narrow spatial distribution include rapid extension of the overlying plate during a megathrust earthquake cycle

Supporting Information:

- Supporting Information S1
- Data Set S1

Correspondence to:

H. P. Johnson,
paulj@uw.edu

Citation:

Johnson, H. P., Merle, S., Salmi, M., Embley, R., Sampaga, E., & Lee, M. (2019). Anomalous concentration of methane emissions at the continental shelf edge of the northern Cascadia margin. *Journal of Geophysical Research: Solid Earth*, 124, 2829–2843. <https://doi.org/10.1029/2018JB016453>

Received 24 JUL 2018

Accepted 11 FEB 2019

Accepted article online 14 FEB 2019

Published online 14 MAR 2019

Anomalous Concentration of Methane Emissions at the Continental Shelf Edge of the Northern Cascadia Margin

H. Paul Johnson¹ , Susan Merle² , Marie Salmi¹ , Robert Embley², Erica Sampaga¹, and Michelle Lee¹

¹School of Oceanography, University of Washington, Seattle, WA, USA, ²NOAA, PMEL EOI program /Oregon State University CIMRS Program, Newport, OR, USA

Abstract A recent compilation of methane plumes detected offshore Washington State includes 1,772 individual bubble streams issuing from 491 discrete vent sites. The majority of these plume sites form a narrow 10-km-wide band located shallower than 250-m water depth, with most sites located near the 175-m-deep continental shelf break that tracks the head scarps of large submarine canyons. Archive multichannel seismic profiles over the Cascadia shelf and uppermost margin that were co-located within a few hundred meters with active emission sites show that methane bubble streams arise from listric/normal faults and triangular-shaped regions of disturbed seismic reflectors that intersect the seafloor and extend several kilometers into the subsurface. Geological processes were evaluated for producing the narrow emission site depths including nonuniform distribution of methane within the Cascadia accretionary sediment wedge and horizontal transfer of groundwater from onshore subaerial sources. A model of enhanced sediment permeability arising from a contrasting response between the inner and outer portions of the accretionary wedge deformation during a megathrust earthquake cycle appears the most likely mechanism. This faulting is generated during extension of the overriding plate during megathrust earthquake cycles, with semicontinuous permeability enhancement of the fluid pathways from excitation by contemporary incident seismic waves.

Plain Language Summary Recognizing individual components of the global carbon cycle is critical to understand both past and present future climates. The sediments that accumulate on continental margins are an underappreciated part of this cycle, containing 40% of the oceanic reservoir of free carbon. Methane plumes issuing from the seafloor are an unquantified leakage of carbon from this giant reservoir. The current inventory of methane plumes on the northern Cascadia margin now approaches 500 emission sites, or an average of one a bubble emission site every 500 m. The majority of these methane emission sites are grouped within a north-south band that follows the continental shelf edge and uppermost margin. The geological process for producing such a narrow band of emissions appears related to the megathrust earthquakes that occur episodically on the Cascadia Subduction Zone that underlies the Washington coast. During these earthquakes, the Juan de Fuca plate is thrust eastward beneath the overlying North American plate. The overlying plate that includes the Washington continental shelf extends rapidly westward during the fault motion. This rapid westward extension of the overlying plate produces faults and diapirs beneath the outer continental shelf, which become pathways for the methane fluid and gas from the margin sediments.

1. Introduction

Almost all continental margins worldwide emit fluid and methane from sediments of the continental shelf and/or the continental slope (Egger et al., 2018). Sediments that accumulate along continental margins play an important role in the global carbon cycle and contain more than 40% of total carbon sequestered within the ocean basins (Muller-Karger et al., 2005). Thus, it seems important to understand the processes responsible for the leakage of mobilized carbon from this large global reservoir. A well-recognized but poorly understood process that transfers mobilized carbon from the interior of continental margin sediments is through the emission of methane, both as gas bubbles and dissolved within the modified pore fluid that escapes from the seafloor (Boetius & Wenzhöfer, 2013; Egger et al., 2018; Hong et al., 2018; Suess, 2014).

A minor portion of this mobilized carbon is immediately captured and returned to the sediment reservoir as solid authigenic carbonate deposits that form directly at the surface of the seafloor by anaerobic oxidation of methane, while the remaining methane is directly transferred to seawater where it is further oxidized to carbon dioxide (Sample et al., 1993; Torres et al., 2002). This study focuses on the 250-km length of the Washington State portion of the Cascadia margin, extending from the Strait of Juan de Fuca to the Columbia River (Figure 1) and uses well-established, acoustic-based geophysical surveys to image methane bubble streams within the water column (Loher et al., 2018). Recent cruises over this NE Pacific sector in the past decade have substantially increased the swath-mapped coverage of the Cascadia accretionary wedge both across- and along-strike, and now include water depths ranging from the shallow continental shelf at less than 100-m water depth to the abyssal plain near 3,000-m depth (Figure 1). Both newly identified and previously published methane emission sites show strong nonuniform depth distribution (Johnson et al., 2015), with the majority of plumes grouped in a narrow band that encompasses the uppermost slope and the adjacent western edge of the continental shelf (Figures 1, 2a and b). Using archive multichannel seismic (MCS) profiles, we correlate plume emission sites to specific subseafloor structures that are visible in the MCS images as a means of identifying possible mechanisms for the plume depth distribution. We then consider several alternative geological processes that could produce this restricted across-strike band of plumes sites. Finally, we suggest a model that attributes the narrow distribution of plume sites near the continental shelf break to faulted and disturbed sediments located at a tectonic boundary between the inner and outer segments of the overlying plate of the main subduction zone fault, segments which have different dynamic behavior during the megathrust earthquake cycle.

2. Washington Margin Geology

The continental shelf and adjacent uppermost slope of the Washington State portion of the Cascadia subduction zone is underlain by a thick section of the Mélange and Broken formation of Eocene to middle Miocene age (MBF; see Snively, 1987; McNeill et al., 1998; McCrory et al., 2002; Campbell et al., 2006 for full descriptions). Coastal outcrops indicate that the MBF is a sheared zone formed of chaotic assemblages of siltstone, sandstone, conglomerate, and altered volcanic blocks. The mechanical weakness and mobility of the MBF geological unit is demonstrated by the slumping of coastal deposits and by the expansive nature of materials encountered by coastal and offshore industry boreholes (Palmer & Lingley, 1989; Rau, 1973). The sheared and discontinuous nature of the MBF produces distorted and chaotic seismic reflections that are in contrast with the overlying younger and well-stratified sediment layers (Figures 2a and 2b).

Beneath the Washington continental shelf, industry boreholes show that MBF extends seaward to the continental shelf edge (Palmer & Lingley, 1989; Rau & Grocock, 1974; Wagner & Batatian, 1986). The upper bound of the formation is located below 700 to 1,000 m of well-stratified sediment layers and the projected but poorly identified bottom of the MBF unit may lie deeper than 4 km (Figures 4a and 4b; Snively, 1987; McNeill et al., 1998). Both seismic profiles and independent evidence from commercial drilling that included the requirement for heavy drilling mud weights indicate that the MBF is permeable, overpressured, and mobile (Palmer & Lingley, 1989; McNeill et al., 1998). The abundant triangular-shaped diapirs visible in seismic profiles on the Washington continental shelf are also largely rooted in the Mélange and Broken formation (Figures 3b, 5a and 5b; Snively & Wagner, 1982; Wagner & Batatian, 1986; Schlische, 1991; McNeill et al., 1998). Examination of Washington coastal fossil outcrops show that the MBF has been associated with methane venting at least since the Miocene (Campbell, 1992; Campbell et al., 2006). Archive multichannel seismic reflection profiles have demonstrated that listric and normal faults with both seaward and landward vergence are widespread on the Washington continental shelf edge and uppermost slopes, (Figures 3a, 3b, 4a, and 4b; also McNeill et al., 1998; McCrory et al., 2002). Fault activity began in the late Miocene and continued into the Holocene, with faults on the continental shelf producing seafloor offsets in modern sediments that are confirmed by video images of exposed outcrops with clean, unsedimented fault faces (McNeill et al., 1998). These listric and normal faults are found both on the continental shelf and uppermost slope, with the more recently active structures located closer to the seaward shelf break (Figure 2a). Most listric faults appear to sole out into a horizontal décollement coincident with the upper portion of the MBF, supporting a direct link between extension and mobility within the MBF (McNeill et al., 1998; Rau & Grocock, 1974; Wagner & Batatian, 1986). It is significant that these listric faults have both alternating landward and seaward vergence, since this style of dual-fault orientation indicates extension by graben

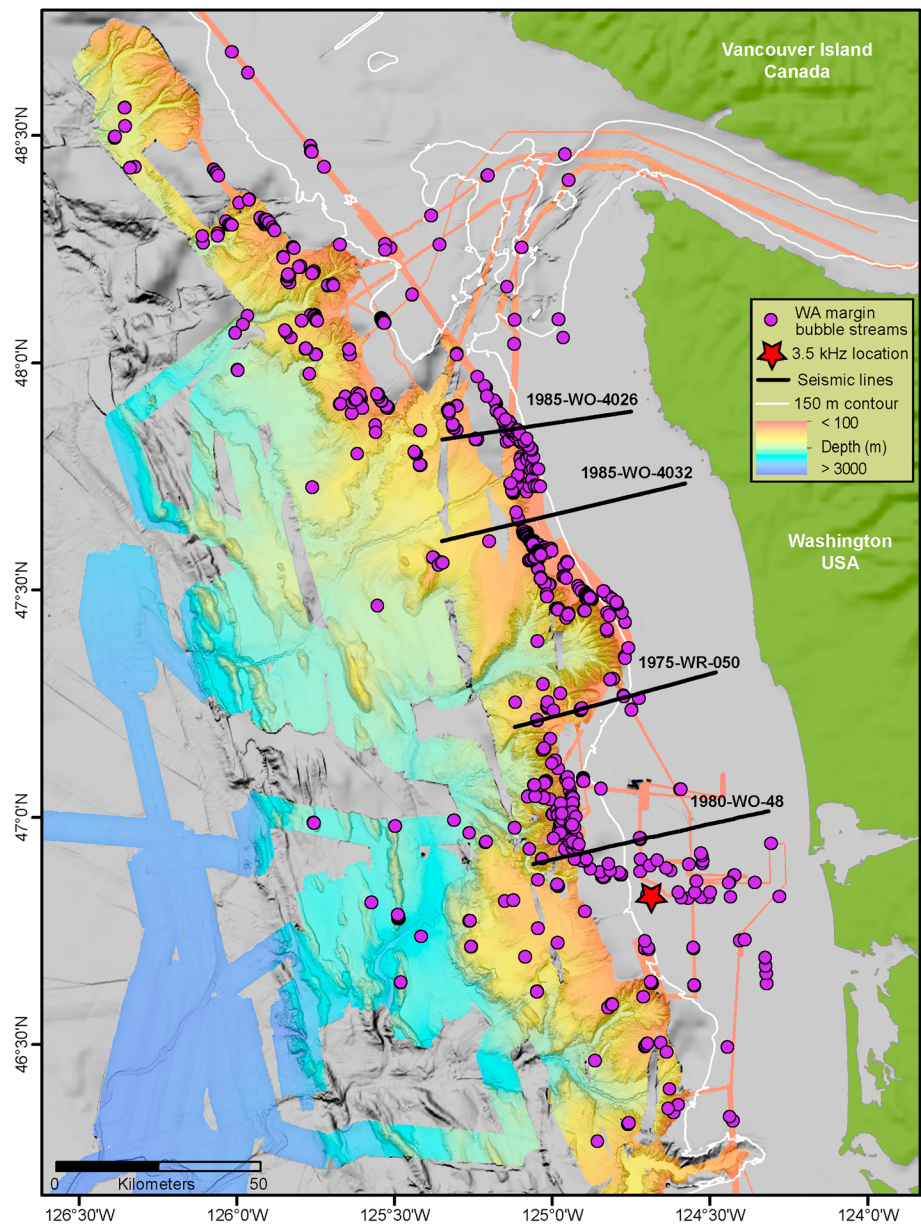


Figure 1. Swath bathymetry map of the areal coverage of the Washington portion of the Cascadia accretionary wedge. Numbers annotating the black lines indicate the archive multichannel seismic profiles shown in the Figures 3a, 3b, 4a, and 4b. Individual bubble stream locations are shown as purple dots. Red star is the location of the 3.5-kHz profile over the shallow mud diapir shown in Figure 5. White contour line is the 150-m depth of the continental shelf edge. Colored areas overlying the gray swath bathymetry map are those areas of the seafloor where water column surveys have been conducted. Emission sites outside the colored swath map were identified by single-channel acoustic profiles. Quileyute Canyon rim lies at the shelf edge between lines 1985-WO-4026 and 1985-WO-4032. The Quinault Canyon rim lies between lines 1985-WO-4032 and 1975-WR-050.

formation, rather than just gravitational collapse of the shelf edge (Illies, 1981; Lister et al., 2018; Schlische, 1991). The archive MCS profiles also show clear growth strata bounded by the normal and listric faults, indicating roughly continuous movement since the Pleistocene or earlier (McNeill et al., 1998; see Figures 3a and 3b).

On the seaward side of the Cascadia accretionary wedge, sediment layers initially deposited horizontally on the abyssal Juan de Fuca plate prior to subduction are folded into landward verging anticlinal ridges from horizontal compression due to the incoming oceanic plate (McCrory et al., 2002; McNeill et al., 1998). In

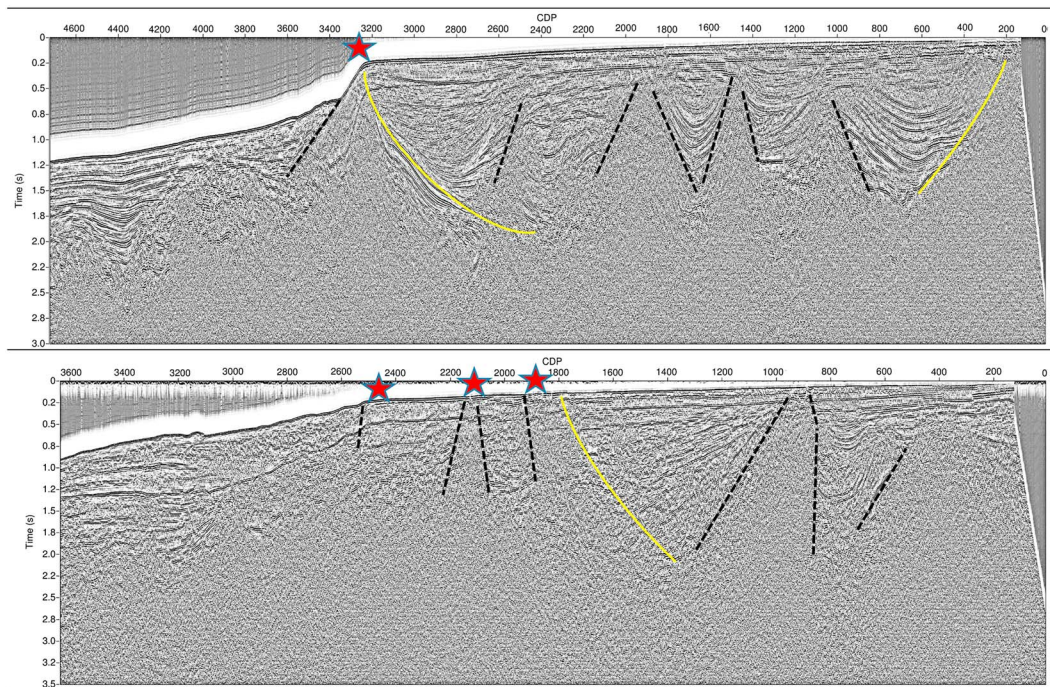


Figure 2. (a) MCS profile 1985-WO-4026 with red stars indicating plume emission sites, yellow lines indicate interpreted listric faults and black dashed lines delineate the boundaries of “wipe-out” zones where the underlying sediment layers are obscured by gas or fluid. See Figure 1 for tracklines. Note the growth structure adjacent to the listric fault, indicating that movement on the extension feature is semicontinuous over time. Water column velocities for all MCS plots are assumed to be 1,450 m/s and 1,700 m/s for sediments on the upper margin (Salmi et al., 2017). (b) 1985-WO-4032. Line interpretations are the same as for (a). Note reversed polarity of the listric faults on the east and west sides of the continental shelf indicating that they formed from horizontal extension, and not simple gravity failure. Black dashed line on left side of shelf edge identifies a slump feature. Some structural features (rollovers, gas pockets, ambiguous reflections) are shown without annotation.

contrast to the continental shelf edge, regions of disturbed sediments located on the lower margin below 500-m water depth do not generally extend to the seafloor and the occurrence of methane bubble emission sites in deep water is sparse (Figures 1, 2, and S1 in the supporting information). On the uppermost margin and western shelf edge, where the regions of distorted sediments and blanked reflectors extend upward to the seafloor, some but not all of the faults become source areas of gas and fluid emissions into the water column (Figures 3a, 3b, 4a, and 4b). This interpretation appears valid for most of the MCS profiles that intersected active emission sites along the full length of the Washington coastal area (Figures S2–S14 in the supporting information).

3. Results

The recent inventory of detected methane bubble streams on the Washington margin exceeds 1,772 individual locations (Figure 1). In the present compilation, multibeam bathymetry surveys that included simultaneous water column plume detection now cover much of the accretionary sediment wedge, ranging from the deep abyssal plain to the continental shelf. Many individual methane bubble streams appear as clusters that surround a central emission site (Johnson et al., 2015; Salmi et al., 2011). To account for possible double-counting of individual bubble streams observed during overlapping surveys, and recognizing that individual bubble streams can be both intermittent in time and active emission orifices can rapidly migrate short distances horizontally (Doya et al., 2017; Hong et al., 2018; Kannberg et al., 2013; Mau et al., 2015; Thomsen et al., 2012), we defined individual emission sites using a previously described clustering method (Johnson et al., 2015). The length of the clustering radii for collecting individual bubble streams into a single emission site was progressively expanded until a 300-m radius from the center of the group was determined to be a characteristic horizontal clustering dimension for plume sites. These clustered bubble plumes are then assumed to have a common subsurface source.

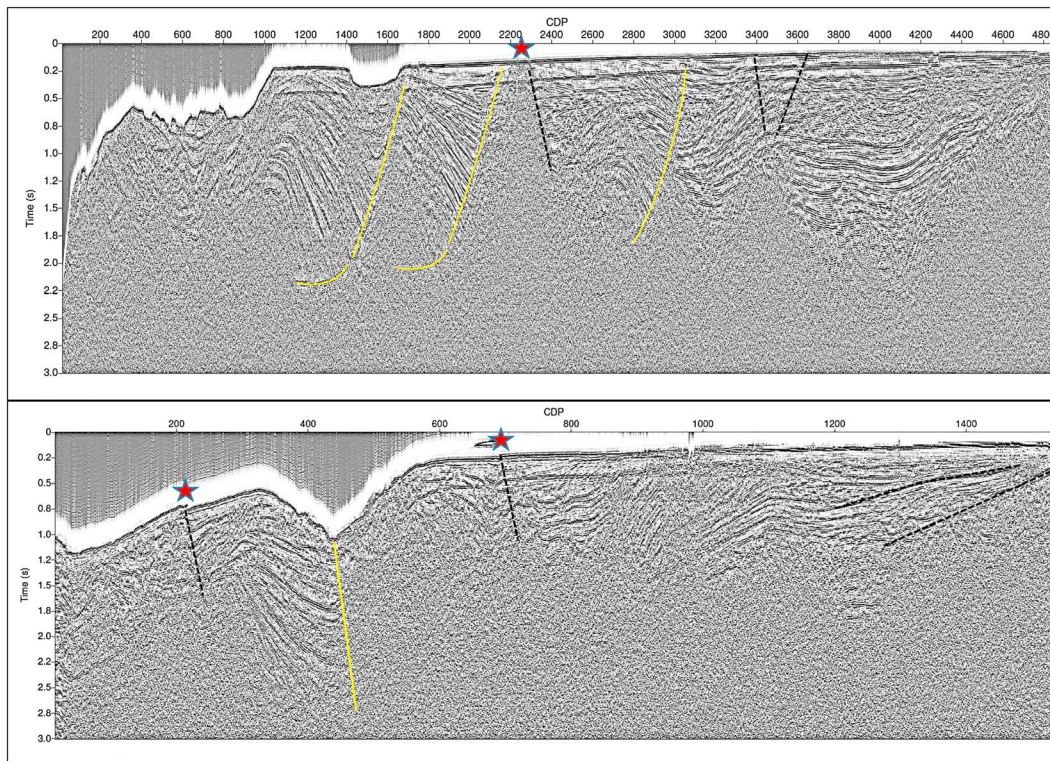


Figure 3. (a) MCS line 1980-WO-48 showing landward verging listric faults (yellow lines) that underlie the methane emission site (red star). Note repetitive growth structures associated with the western (left) faults. Linear reflections can present as curved lines due to changes in the seismic velocity within the sediments, and this possibility is ignored in the following MCS images. (b) MCS line 1975-WR-50, showing similar features to (a), but with a plume emission site seaward of the shelf edge on left side of diagram that is associated with a fault and growth structure. Note the offset of the seafloor below the emission site at location CDP 700.

In the present inventory, this plume-clustering method resulted in 1,772 observed bubble streams being grouped into 491 individual emission sites which can be seen by comparison of the distributions in Figures 1 and S1 in the supporting information. Although methane plumes can be found at all water depths on the Cascadia accretionary wedge, the majority of these sites are located at the western edge of the continental shelf and uppermost margin slope, within a narrow water depth range from 100 to 250 m, a range which includes 74% of observed bubble streams locations and 56% of the clustered emission sites (Figure 4).

4. Models for Emission Site Depths

The observed concentration of methane/fluid emission sites within an E-W band located at the boundary between the Cascadia lower margin and continental shelf edge requires consideration of possible geological processes responsible for this distribution. These interpretations must include the caveat that only a small area of the shallow continental shelf has been surveyed. Because of the incomplete nature of available data required to unequivocally identify the geological processes responsible for the methane/fluid emissions on the Washington margin, we employ the methodology of “multiple working hypotheses” described by Chamberlin (1890) and Elliott and Brook (2007). In this strategy, we evaluate alternative hypotheses and then identify our preferred model. A summary of potential processes includes (1) the Null Hypothesis of random distribution of sites, (2) a nonuniform distribution of the subsurface reservoirs of methane contained within the accretionary wedge, (3) horizontal flow within a subsurface aquifer of fluid from a terrestrial reservoir, and (4) localized enhanced sediment permeability arising from shaking by regional and distant earthquake waves. We then describe our preferred model of differential tectonic movement resulting from the dynamic response of the accretionary wedge to the full megathrust earthquake cycle proposed previously for Cascadia (Hyndman & Wang, 1993; McNeill et al., 1998) and for subduction zone sediment prisms in general (von Huene et al., 2004; Wang et al., 2012; Wang & Tréhu, 2016). Although none of these five alternatives has compelling supporting data, we describe our preference for the differential tectonic response

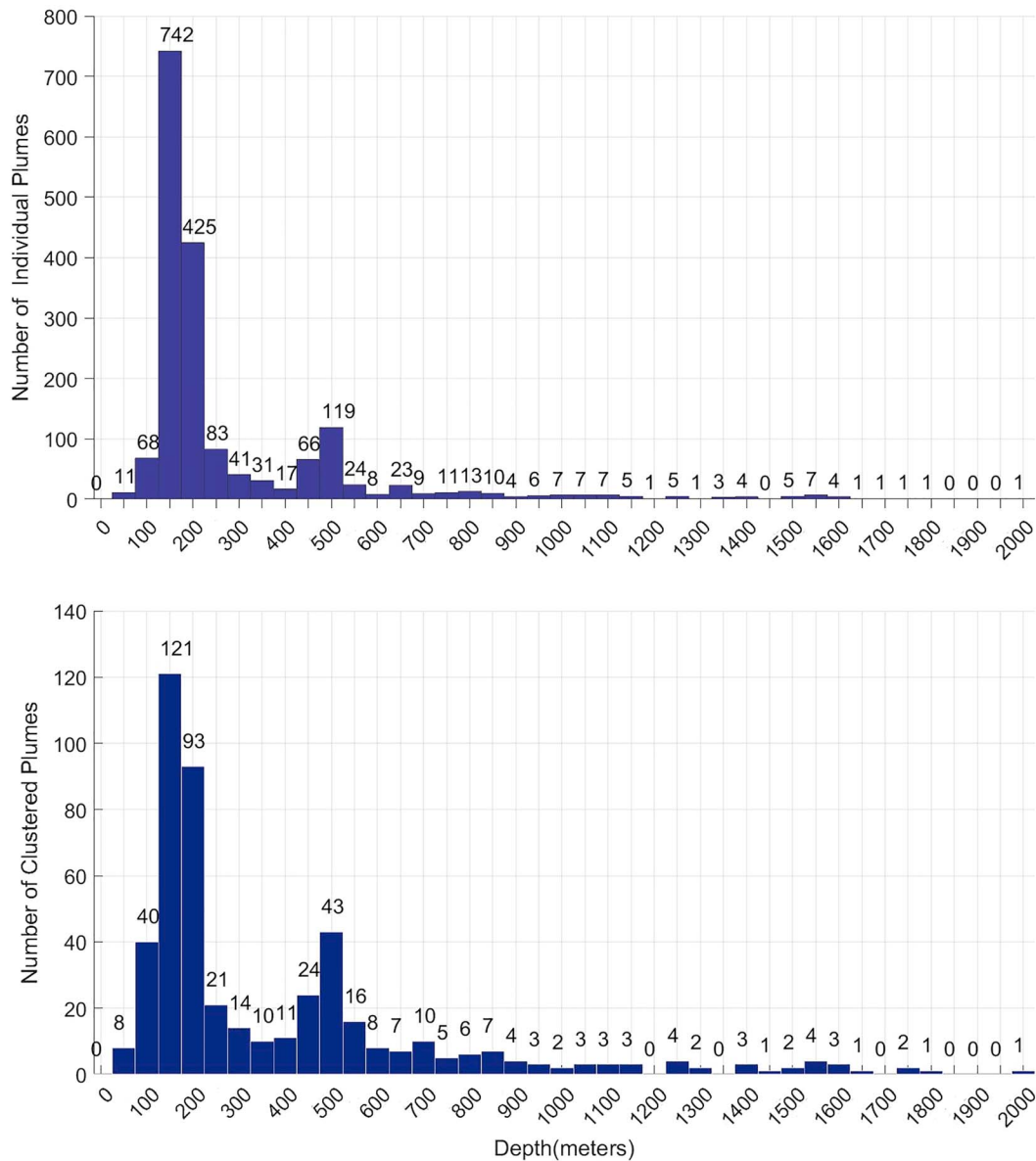


Figure 4. (a) Histogram of the depth distribution for individual bubble stream emission sites, binned in 50-m depth intervals without any clustering method applied. Note the peak in depth at approximately 175-m water depth, and a secondary peak at 500-m water depth. (b) Depth distribution histogram of methane emission sites where a 300-m clustering radius has been applied.

model as the most plausible cause of the unusually narrow methane emission site distribution on the Washington continental shelf.

4.1. Null Hypothesis: Uniform Seep Distribution

The Null Hypothesis regarding the depth distribution of methane plume emissions argues that these sites should be either uniformly or randomly distributed over the entire accretionary wedge, from the deformation front at abyssal depths to the coastline. Although a prominent feature from Figure 1 is the lack of extensive survey coverage over much of the continental shelf due to the shallow depth and narrow acoustic swaths, the Null Hypothesis is difficult to support given the site depths and distributions shown in Figures 1, 4a, and 4b. Prior modeling studies of Cascadia margin dynamics suggested that the maximum dewatering of the accretionary wedge should occur within the lower margin, in deep water near 2,800-m water depth, and located only 15 to 30 km landward from deformation front (Kastner et al., 2014; Saffer

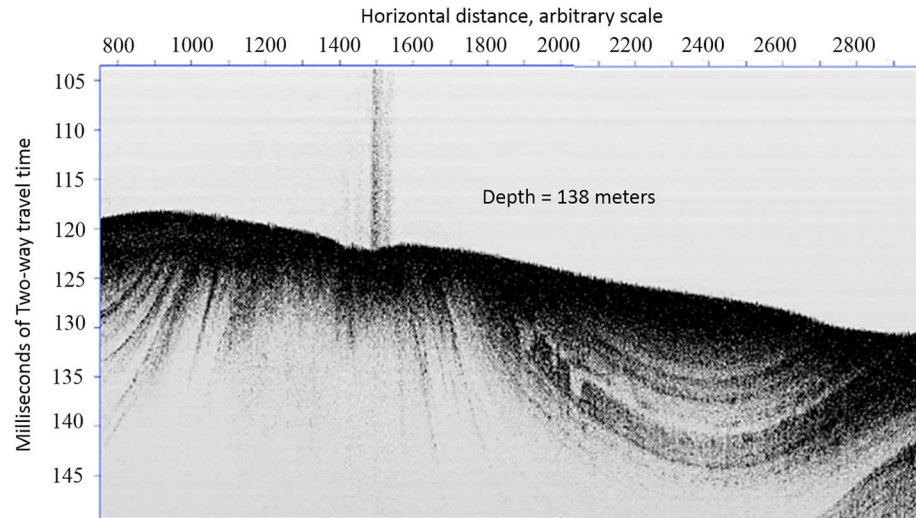


Figure 5. Profile shows 3.5-kHz acoustic image of the methane plume site shown as the red star on Figure 1. Near surface stratigraphy indicates upwelling of diapir-like structure associated with methane plume site. Bubble stream issues from shallow pock-mark seen in surface contour. Methane emissions are shown by vertical bubble reflections.

et al., 2008; Wang et al., 1993). The majority of fluid emitted from the lower portion of the accretionary wedge has been attributed to fluid generated from both clay dehydration and the Opal-A/Opal-C conversion to quartz, rather than simple compression of sediment pores during accretionary wedge formation (Hyndman et al., 1993; Saffer et al., 2008; Wang et al., 1993).

Comparison of structures visible within the archive MCS profiles that are co-located with presently active methane vent locations illustrates that seafloor regions directly beneath the emission sites consist of disturbed sediments that are roughly triangular-shaped, with the narrow apex at the site of seafloor emissions (Figures 3a and 3b). This type of “zonal blanking” of sediments has been attributed to (a) acoustic attenuation due to fluid flow, (b) the presence of free gas, and/or (c) the mechanical disturbance of the original horizontal sediment layering and are normally considered piercement structures or diapirs (Judd & Hovland, 1992; Rau & Grocock, 1974; Riedel et al., 2002). For the full 250-km north-south length of the Washington margin of this study, there appears to be a positive association between the locations of methane emission sites and the roughly diapir-shaped segments of disturbed sediments in the subsurface and areas of normal and listric faulting. This qualitative correlation appears to be consistent for many of the archive MCS and single-channel profiles (Figures 5 and S2–S12 in the supporting information).

The relationship between regions of disturbed seafloor reflectors and both listric and normal faults with sites of fluid/gas emissions for subduction zone margins has been noted in previous studies (Li et al., 2013; Rau & Grocock, 1974; Spence et al., 1995; Wagner & Batatian, 1986; Yuan et al., 1994, 1996). However, the converse is not true. While all emission sites with overlying MCS profiles appear to be underlain regions of seismic blanking or faulting, not all areas of disturbed/blanked sediments in the MCS profiles or visible faults produce gas/fluid emission sites that were currently active during the intervals of the acoustic water column surveys. This lack of full two-way correlation is likely due to an absence of fluid flow within older fault channels, the intermittency of gas emissions, or the simple lack of complete survey coverage. Due to the configuration of the ship-based acoustic beam, identification of water column reflectors is difficult and substantially less efficient at the edge of the swath, even when producing near-100% bathymetry coverage.

4.2. Nonuniform Distribution of Methane Within the Accretionary Wedge

Another possibility for the narrow cross-strike distribution of methane emission sites would occur when acoustically visible bubble plumes in the water column are present only where there is an overpressured reservoir of mobile methane located directly below or in the immediate vicinity of the venting from the seafloor. This hypothesis requires that methane gas reservoirs should exist primarily within the seafloor

sediment of the Cascadia slope directly beneath the western boundary of the WA continental shelf, where the majority of bubble streams occur. Thus, subsurface methane reservoirs would have to be generally absent from the deeper portions of the accretionary wedge, where plumes are rarely found. A limited test of this hypothesis is to exam the potential for correlation between the presence of bottom simulating reflectors (BSRs), which are clear indicators of the presence of gas and solid phase methane hydrate, and the locations of active bubble plume emission sites. At the latitude of the Washington State margin, the seafloor sediments are too shallow directly beneath the continental shelf edge at 175-m water depth to produce BSRs, as the upper hydrate stabilization depth is at 490-m depth (Hautala et al., 2014).

BSRs have been extensively mapped on the Cascadia accretionary prism using active source MCS surveys. These reflectors appear widely distributed both across- and along-strike of the accretionary wedge, extending from Mendocino in northern California to Vancouver Island. A recent compilation by Phrampus et al. (2017) found that there is a significant gap in the distribution of BSRs along-strike of Cascadia upper margin occurs within the Washington segment, between the latitudes 47°N and 48°N, although many of the MCS profiles examined do not extend to the accretionary toe. This is a region where methane bubble stream emissions are particularly abundant on the upper margin and at the continental shelf edge (Figures 1 and S1 in the supporting information). These combined observations suggest the interpretation that the emission of methane/fluid from the seafloor and the presence of subseafloor BSRs are independent manifestations of subsurface methane distribution. This conclusion is supported by previous studies demonstrating that the hydrate/gas interface is present, even when the BSR is not observed in seismic profiles (e.g., Holbrook et al., 2002).

4.3. Terrestrial Aquifer Transfer

Another explanation of the narrow depth distribution of bubble plumes is a model where the source of methane/fluid in the emissions at the shelf edge arises from the horizontal movement of terrestrial groundwater flowing through shallow subsurface aquifers located beneath the continental shelf. In this alternative, the terrestrially sourced fluid re-emerges as low-salinity springs from outcrops seaward of the coastline (Faure et al., 2002; Orange et al., 1999; Post et al., 2013; Puig et al., 2017). Fresh groundwater discharge into nearshore seawater environments has been shown previously to contribute to the physical and chemical environment of some restricted coastal waters, but the role of coastal groundwater at the larger regional to continental scales remains poorly defined (Befus et al., 2017; Michael et al., 2005).

The exposure of the relatively high-permeability Melange and Broken formation on the Washington portion of the Cascadia margin represents a possible geological unit that could serve as a horizontal aquifer of terrestrial-sourced fluid (Campbell et al., 2006). However, the north-south extent of the Melange and Broken formation exposure is limited to a relatively narrow portion of the northernmost part of the Olympic Peninsula (Campbell, 1992; McNeill et al., 1998), while the observed band of methane plume emissions at the shelf edge extends to both southern Washington and likely farther south into central Oregon (Figure 1; Johnson et al., 2015). Further problems with this alternative hypothesis is that the nearest subaerial recharge zone for the MBF is located approximately 60 km east of the shelf-edge emissions sites (Figure 1).

4.4. Seismic Energy Shaking at Edge of Continental Shelf Break

A further process that may contribute the narrow band of methane plume sites arises from their location near the sharp topographic break in seafloor slope that forms the western edge of the continental shelf edge. Sharp slope inflections of the seafloor have been recognized previously as localized areas that produce enhanced fluid emissions (Kukowski et al., 2010; Orange et al., 1999). Local geologic structures and surface topography are also known to amplify seismic waves from distant sources, and as a result, enhance sediment permeability in both the terrestrial environment (Roeloffs, 1998) and on accretionary prisms (Hammerschmidt et al., 2013). A recent study of the seismic site response of ocean bottom seismometers on the Cascadia accretionary wedge demonstrated that seismic shaking at low excitation frequencies that occur near the continental shelf break are both amplified in intensity by 2 orders of magnitude and substantially prolonged in duration by the presence of a substantial change of slope (Gomberg, 2018). This phenomenon has been proposed to increase the permeability of upper slope and shelf-edge sediments, which would enhance bubble transfer from the subsurface reservoir.

On Cascadia, abundant methane plumes appear associated with the heads of steep marginal canyons, with the Quinault and Quileute Canyons as examples (Figures 1 and S1). Other North American submarine canyons located on passive rather than active margins also have shown clusters of plume emission sites, although these vent sites are primarily located within deep canyon thalwegs and are generally absent from the steep slopes of the canyon walls or heads (e.g., Barry et al., 1996; Weinstein et al., 2016). It is important to note that the Quinault Canyon head, with an abundance of emission sites, has a striking vertical relief of approximately 1,000 m (Figure 1). The seismic site response amplification recorded by Cascadia ocean bottom seismometers at low seismic frequencies (Gomberg, 2018) requires dynamic participation of the entire thickness of the accretionary wedge from the seafloor to igneous oceanic plate, which lies at a vertical distance of 20 km below the shelf edge at Quinault Canyon (McCrorry et al., 2012).

For comparison with other topographic changes of similar scale within the Washington accretionary wedge, the abyssal hills arising from anticlinal ridges on the lower margin of the Quinault area have vertical relief on the order of 300 to 400 m and the sediment wedge is only 5 to 7 km in thickness (McCrorry et al., 2012). However, this scale of topographic relief on the lower accretionary wedge shows little seismic wave amplification in ocean bottom seismometer instrumentation (Gomberg, 2018). The same lower to middle-slope region of the accretionary wedge contains well-defined BSRs within the anticlinal ridges, but the area is not a major source of methane bubble streams (Figure 1; Salmi et al., 2017). This suggests that enhanced sediment permeability at the seaward boundary of the continental shelf that results from the relationship between topographic slope, thickness of the accretionary wedge, and the frequency of seismic wave energy from distal earthquakes is a likely real phenomenon (Gomberg, 2018), but the exact mechanism and resulting impact on permeability is still undefined.

4.5. Tectonic Response to Megathrust Earthquakes

As our preferred model, we suggest that discrete portions of the northern Cascadia accretionary margin respond differently during the seismic and interseismic portions of a full earthquake cycle, and this difference in tectonic response produces a faulted and highly permeable expansion zone that is responsible for the observed narrow band of methane emissions. Our conceptual model for the origin of the horizontal extension zone located at the continental shelf edge and uppermost slope of the Washington margin is based on the original structural observations of Hyndman and Wang (1993) and McNeill et al. (1998). Subsequent models of the horizontal extension that occurs to the overlying plate during a full megathrust earthquake cycle also have been published previously (e.g., Plafker, 1969; von Huene et al., 2004), and more recently extended and modeled by Wang et al. (2012).

Wang et al. (2012) suggested that multiple tectonic motions are present during a subduction zone rupture which include (1) the interseismic compression of the accretionary wedge from the incoming oceanic plate, (2) the abrupt seaward extensional thrust of the overlying plate during the coseismic period, (3) the rapid relocking of the décollement fault, and (4) a period of delayed afterslip where the seaward motion of the original fault continues in the hanging wall within a zone located just landward of the fully locked zone. In this model of the megathrust earthquake cycle, the immediate postseismic movement of the narrow afterslip zone is responsible for the extension structures that are prominent at the continental shelf and uppermost slope, which in the present study are represented by the band of listric/normal faults and diapirs in the MCS profiles (Figure 5). In our interpretation, these faults and diapirs provide the high-permeability pathways that allow vertical transfer of fluid from the overpressured MBF formation that lies below the stratified sediment layers, producing the plume distribution visible in Figures 1 and 2.

A local modification to this tectonic model is suggested by the presence of the overpressured and highly mobile Mélange and Broken formation on the Washington margin (Figure 6; Palmer & Lingley, 1989; McNeill et al., 1998). The mobile, high-permeability, and sheared nature of this geological unit suggests that the MBF mechanically decouples the overlying well-stratified and relatively undisturbed sediments from the elastic response of the underlying upper plate below the MBF (Figure 6). In this case, the seaward motion that occurs during the period of the megathrust afterslip produces the extension recorded in the listric/normal faulting and the upward migration of gas-rich diapirs from the overpressured MBF formation below. The extension in the overlying plate then produces the vertical permeability that promotes the formation of a narrow band of methane and fluid emissions at the uppermost margin and the seaward continental shelf edge.

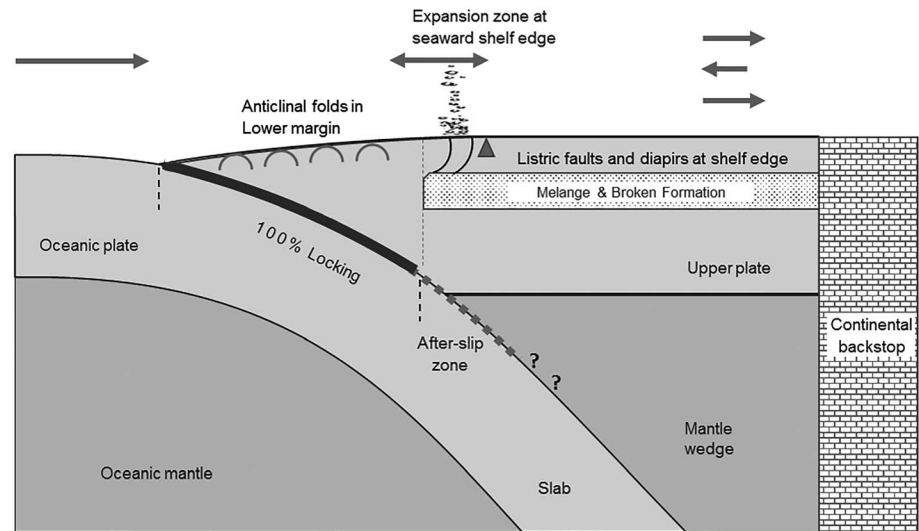


Figure 6. Schematic diagram showing the multiple stages of tectonic deformation that produce faulted zones of permeable pathways that provide the deep source of gas and fluid that are the source area of the bubble plumes. Figure is adapted from Wang et al. (2012), but modified to include the Mélange and broken formation. Stages in the earthquake cycle that produce the expansion zone at the western edge of the continental shelf and uppermost accretionary margin are described in the text. Arrows show the tectonic behavior during the full reversal of a megathrust earthquake cycle for the western shelf edge and uppermost continental slope. Vertical or horizontal axes are to not to scale.

Location of the downdip boundary of the 100% locked portion Cascadia subduction zone is an important component to this tectonic model. Several independent methods have been used to identify the downdip boundary of the seismogenic zone for the Cascadia Margin, including thermal data and modeling (Hyndman et al., 1997; Hyndman & Wang, 1995), geodetic data derived from GPS stations (McCaffrey, 2009), coastal subsidence models (Wang et al., 2013), and numerical models incorporating observational geophysical data as boundary conditions (Olsen et al., 2008; Wang et al., 2003). Recently, Bruhat and Segall (2016) used a compilation of GPS geodetic data and a tidal model that placed this downdip boundary of the fully locked zone at the continental shelf edge for the Washington State portion of the Cascadia margin.

A recent revision of the thermal model positions the downdip limit of the fully locked/seismogenic zone along the décollement at the 350 °C isotherm, which for the Washington margin also places it directly beneath the continental shelf break (Salmi et al., 2017). In this thermal model, the interval between 350 °C and 450 °C for décollement temperatures represented the partially locked transition zone (Hyndman et al., 1997; Oleskevich et al., 1999), a region which Wang et al. (2012) also assign as the updip limit of the zone of afterslip in the full megathrust earthquake cycle. Wang et al. (2012) propose that the motions produced by the megathrust earthquake, specifically including the seaward motion of the overlying hanging wall, continue for months within the afterslip zone after the initial breaking and healing of the primary locked zone. Based on the collective results described above that are derived from diverse data sets but still arrive at a common downdip boundary of full locking of the décollement, we hypothesize that the western edge of the Washington continental shelf and the uppermost margin overlies the landward edge of the velocity-weakening (i.e., fully locked, seismogenic) portion of the décollement that separates the outer accretionary wedge from the uppermost slope and continental shelf portion of the wedge. This segment continues the seaward motion of the hanging wall during the afterslip period and is responsible for the E-W extension of the sediment layers that overlie the MBF and the uppermost slope and continental shelf edge (Figure 6).

Listric and normal faults likely play a similar role in transporting fluid from deep within the accretionary wedge on the upper Cascadia margin as they do in other subduction zones (e.g., Hensen et al., 2004; Melnick et al. 2012; Moore & Saffer, 2001). These quasi-vertical faults have been shown to be conduits for gas, fluid, and solute, transporting a high percentage of the total dewatering flux from deep in the accretionary wedge to the overlying seafloor, and in doing so, weaken and segment the upper plate (Lauer & Saffer, 2015). Although the MCS reflections we are interpreting as listric and normal faults are not visible in all of

the archive along-strike MCS images, most profiles demonstrate that the uppermost margin and western continental shelf edge is a zone that has experienced extension, including placement of subsurface diapirs and tectonic disturbances that are co-located with active bubble plume emissions (Figures 2a, 3a, 3b, and S2–S12 in the supporting information).

4.6. Methane Plume Sites at 500-meter Water Depth

The smaller methane plume site depth peak present at approximately 500-m water depth requires further discussion (Figures 2a and 2b). Previous studies have suggested that anthropogenic seawater-induced warming destabilizes the upper feather edge of solid hydrate deposits, producing a clustering of methane plumes that occurs at 500-m water depth (Hautala et al., 2014; Johnson et al., 2015). The interpretation of methane plumes arising from modern seawater warming requires that the observed methane emission sites have become active only within the past few decades, during the period of anthropogenic seawater warming. The recent ROV observations of large carbonate slab deposits located around some but not all of the Cascadia plumes at the 500-m water depth has added complexity to this argument (Embley et al., 2016). These carbonate structures on the seafloor grow at rates of less than a centimeter per 1,000 years (Bayon et al., 2009), and therefore, the 10- to 20-cm-thick slabs that are sometimes visible at these 500-m-deep sites cannot have been recent accumulations. The origin of the plume site depth peak at 500-m water depth is still unresolved, particularly since any explanation must account for the large but slowly accumulating carbonate deposits that surround many of these emission sites.

5. Conclusions

The present inventory of acoustically detected methane bubble streams on the Washington portion of the Cascadia margin totals 491 distinct gas and fluid emission sites distributed at all depths along the accretionary wedge, ranging from the deformation front to the shallow continental shelf. Surprisingly, the plume sites have a restricted depth dependency, with the majority lying between 100- and 250-m water depth and located on the uppermost shelf and near the western boundary of the continental shelf. The relatively narrow band of fluid and gas emission sites on the Cascadia margin is correlated with presence of subseafloor acoustic reflectors characteristic of listric/normal faults and disturbed/blanked sediment diapir-like intrusions that intersect the seafloor directly at the fluid emission sites. These fault zones and intrusion sites provide the required pathways for subsurface fluid and methane transport from deep within the margin sediments. This correlation between plume sites, faults, and diapirs suggests that the source area for the methane and fluid emissions lies within the deeper subsurface below 1 km and is likely to be derived from clay and opal dehydration reactions within the Mélange and Broken formation, a geophysical prediction that requires a geochemical test of the emission fluid.

Zones of across-strike extension have been found on the overriding plate of subduction zones for both accretionary (Wang & Hu, 2006) and erosional subduction margins (Plafker, 1969; von Huene et al., 2004), but the presence of the overpressured and permeable MBF as the source region of abundant methane emissions may be a phenomenon local to the Washington segment of the Cascadia accretionary wedge. A simple test of the generalization of our model would be to examine the depth distribution of methane emissions on the Oregon portion of Cascadia, where methane plumes are also found (Johnson et al., 2015; Torres et al., 2009) and the subsurface Mélange and Broken formation is not present (McNeill et al., 1998), but the subduction zone environment is still similar to that in the north.

It is also important to note that while other subduction zones show fluid emissions from structural boundaries within the overlying plate (Geersen et al., 2016; Kukowski et al., 2010; Melnick et al., 2012; Tsuji et al., 2015), those location-specific tectonic boundaries between the inner and outer margins are found in deeper water, rather than at the shallow Cascadia continental shelf edge. For these margins, the location of the deeper structural boundary may be controlled by parameters other than the downdip limit of the local seismic zone and afterslip region.

In summary, all of the models presented here may be tested with future field and laboratory investigations. As with all scientific models, the most viable hypothesis may lie with an alternative that is still unrecognized. It is clear that a continuing examination of the relationship among fluid and methane flux, temporal variations in tectonic response of the overlying plate, and the location of the 100% locked zone of the

décollement is a fertile field for study. Although quantitative estimates for the amount of fluid flux emitted from this zone of the upper accretionary wedge has only been roughly estimated (Riedel et al., 2018), the relative number of visible bubble streams in northern Cascadia may ultimately demonstrate that mobilized carbon leaking from subduction zone margins may yet prove to be a significant component of the global carbon cycle (Dean et al., 2018).

6. Methods

Our compilation of the Cascadia accretionary wedge methane plume sites offshore Washington State have used two distinct acoustic detection methods: (1) single beam subbottom profiler with either specific (3.5 kHz) or variable frequency chirp systems, and higher-frequency (50 to 200 kHz) fish-finders for sites volunteered by local fishermen (Johnson et al., 2015). (2) The second method for plume detection uses multi-beam echo sounder systems that collect simultaneous seafloor and water column data. Data from the multi-beam echo systems used in this study include the R/V *Thompson* TN265 and TN314 (EM302; 30 kHz); R/V *Atlantis* Cruise 18-09 (EM122; 12 kHz); the E/V *Nautilus* NA072, NA078, and NA080 (EM302; 30 kHz); and NOAA Ship Rainier Cruise 1605 (EM710; 70 to 100 kHz). The range of water depths for these systems reach beyond the 3,600-m maximum depth of the NE Pacific except for the Rainier/EM710 which was limited to depths shallower than 1,000 m. Bubble plumes present within the water column were identified using commercial acoustic signal processing software, either Fledermaus© or CARIS©. The image processing methodology used for swath bathymetry data has been described in previous studies (Hautala et al., 2014; Johnson et al., 2015). The swath bathymetry data obtained by individual research cruises that contributed to this plume compilation are shown in Figure 1. Due to the inefficiency of capturing water column reflectors at the edge of the acoustic beam, bubble plumes can go undetected even when the swath bathymetry is producing 100% coverage of the seafloor. This suggests that the number of bubble streams detected by any bathymetric survey remains undercounted.

An important caveat for this plume inventory is the obvious scarcity of survey lines located directly on the shallow continental shelf (<150 m). This shallow seafloor has limited swath bathymetry survey coverage due to the narrowing of the acoustic beam width from the shallow depths, although the compilation contains some limited single beam and fish-finder plume data from obtained from volunteer fishermen (Johnson et al., 2015).

Acknowledgments

Archive multichannel seismic profiles used in this study are publically available from the following U.S. Geological Survey websites: 1975: <https://walrus.wr.usgs.gov/namss/survey/w-18-75-np/>, 1980: <https://walrus.wr.usgs.gov/namss/survey/w-29-80-wo/>, and 1985: <https://walrus.wr.usgs.gov/namss/survey/w-39-85-wo/>. Langseth Line 5 data are publically available from the National Geophysical Data Center or GeoPRISM website (COAST 2012: <http://www.marine-geo.org/tools/search/entry.php?id=MGL1212>) or from <https://catalyst.uw.edu/workspace/paulj/17643/363717>. Line 5 of the Langseth COAST survey was commercially processed postcruise, and the details are described in Salmi et al. (2017). NSF grant 1634095 was provided to H.P.J.; helpful reviews were provided by Brian Atwater and Christian Ballard. Peter Lathourakis is acknowledged for his help in sending methane plume locations from his commercial fishing expeditions. Additional MCS profiles are contained in the supporting information along with an Excel file of the methane emission site locations. NOAA contributed to this study (contribution PMEL 4866).

References

- Barry, J. P., Greene, H. G., Orange, D. L., Baxter, C. H., Robison, B. H., Kochevar, R. E., et al. (1996). Biologic and geologic characteristics of cold seeps in Monterey Bay, California. *Deep Sea Research Part I: Oceanographic Research Papers*, 43(11–12), 1739–1762.
- Bayon, G., Henderson, G. M., & Bohn, M. (2009). U–Th stratigraphy of a cold seep carbonate crust. *Chemical Geology*, 260(1–2), 47–56. <https://doi.org/10.1016/j.chemgeo.2008.11.020>
- Befus, K. M., Kroeger, K. D., Smith, C. G., & Swarzenski, P. W. (2017). The magnitude and origin of groundwater discharge to eastern U.S. and Gulf of Mexico coastal waters. *Geophysical Research Letters*, 44, 10,396–10,406. <https://doi.org/10.1002/2017GL075238>
- Boetius, A., & Wenzhöfer, F. (2013). Seafloor oxygen consumption fueled by methane from cold seeps. *Nature Geoscience*, 6(9), 725–734. <https://doi.org/10.1038/ngeo1926>
- Bruhat, L., & Segall, P. (2016). Coupling on the northern Cascadia subduction zone from geodetic measurements and physics-based models. *Journal of Geophysical Research: Solid Earth*, 121, 8297–8314. <https://doi.org/10.1002/2016JB013267>
- Campbell, K. A. (1992). Recognition of a Mio-Pliocene cold seep setting from the Northeast Pacific convergent margin, Washington, U.S.A. *PALAIOS*, 7(4), 422–433. <https://doi.org/10.2307/3514827>
- Campbell, K. A., Nesbitt, E. A., & Bourgeois, J. (2006). Signatures of storms, oceanic floods and forearc tectonism in marine shelf strata of the Quinault formation (Pliocene), Washington, USA. *Sedimentology*, 53(5), 945–969. <https://doi.org/10.1111/j.1365-3091.2006.00788.x>
- Chamberlin, T. C. (1890). The method of multiple working hypotheses. *Science*, 15, 92–96.
- Dean, J. F., Middelburg, J. J., Röckmann, T., Aerts, R., Blauw, L. G., Egger, M., et al. (2018). Methane feedbacks to the global climate system in a warmer world. *Reviews of Geophysics*, 56, 207–250. <https://doi.org/10.1002/2017RG000559>
- Doya, C., Chatziveangelou, D., Bahamon, N., Pursler, A., De Leo, F. C., Juniper, S. K., et al. (2017). Seasonal monitoring of deep-sea megabenthos in Barkley Canyon cold seep by internet operated vehicle (IOV). *PLoS One*, 12(5), e0176917. <https://doi.org/10.1371/journal.pone.0176917>
- Egger, M., Riedinger, N., Mogollón, J. M., & Jørgensen, B. B. (2018). Global diffusive fluxes of methane in marine sediments. *Nature Geoscience*, 1.
- Elliott, L. P., & Brook, B. W. (2007). Revisiting Chamberlin: Multiple working hypotheses for the 21st century. *AIBS Bulletin*, 57(7), 608–614.
- Embley, R. W., Merle, S. G., Raineault, N., Baumberger, T., Seabrook, S., Johnson, H. P., et al. (2016), February. Numerous bubble plumes mapped and new seeps characterized on the Cascadia margin. In *AGU Fall Meeting Abstracts*.
- Faure, H., Walter, R. C., & Grant, D. R. (2002). The coastal oasis: Ice age springs on emergent continental shelves. *Global and Planetary Change*, 33(1–2), 47–56. [https://doi.org/10.1016/S0921-8181\(02\)00060-7](https://doi.org/10.1016/S0921-8181(02)00060-7)

- Geersen, J., Scholz, F., Linke, P., Schmidt, M., Lange, D., Behrmann, J. H., et al. (2016). Fault zone-controlled seafloor methane seepage in the rupture area of the 2010 Maule earthquake, central Chile. *Geochemistry, Geophysics, Geosystems*, *17*, 4802–4813. <https://doi.org/10.1002/2016GC006498>
- Gomberg, J. (2018). Cascadia onshore-offshore site-response, submarine sediment mobilization, and earthquake recurrence. *Journal of Geophysical Research: Solid Earth*, *123*, 1381–1404. <https://doi.org/10.1002/2017JB014985>
- Hammerschmidt, S., Davis, E. E., & Kopf, A. (2013). Fluid pressure and temperature transients detected at the Nankai Trough megasplay fault: Results from the SmartPlug borehole observatory. *Tectonophysics*, *600*, 116–133. <https://doi.org/10.1016/j.tecto.2013.02.010>
- Hautala, S. L., Solomon, E. A., Johnson, H. P., Harris, R. N., & Miller, U. K. (2014). Dissociation of Cascadia margin gas hydrates in response to contemporary ocean warming. *Geophysical Research Letters*, *41*, 8486–8494. <https://doi.org/10.1002/2014GL061606>
- Hensen, C., Wallmann, K., Schmidt, M., Ranero, C. R., & Suess, E. (2004). Fluid expulsion related to mud extrusion off Costa Rica—A window to the subducting slab. *Geology*, *32*(3), 201–204. <https://doi.org/10.1130/G20119.1>
- Holbrook, W. S. A., Gorman, R., Hornbach, M., Hackwith, K. L., Nealson, J., Lizarralde, D., & Pecher, I. A. (2002). Seismic detection of marine methane hydrate. *The Leading Edge*, *21*(7), 686–689. <https://doi.org/10.1190/1.1497325>
- Hong, W. L., Torres, M. E., Portnov, A., Waage, M., Haley, B., & Lepland, A. (2018). Variations in gas and water pulses at an Arctic seep: Fluid sources and methane transport. *Geophysical Research Letters*, *45*, 4153–4162. <https://doi.org/10.1029/2018GL077309>
- von Huene, R., Ranero, C. R., & Vannucchi, P. (2004). Generic model of subduction erosion. *Geology*, *32*(10), 913–916. <https://doi.org/10.1130/G20563.1>
- Hyndman, R. D., & Wang, K. (1993). Thermal constraints on the zone of major thrust earthquake failure: The Cascadia subduction zone. *Journal of Geophysical Research*, *98*(B2), 2039–2060. <https://doi.org/10.1029/92JB02279>
- Hyndman, R. D., & Wang, K. (1995). The rupture zone of Cascadia great earthquakes from current deformation and the thermal regime. *Journal of Geophysical Research*, *100*(B11), 22,133–22,154. <https://doi.org/10.1029/95JB01970>
- Hyndman, R. D., Wang, K., Yuan, T., & Spence, G. D. (1993). Tectonic sediment thickening, fluid expulsion, and the thermal regime of subduction zone accretionary prisms: The Cascadia margin off Vancouver Island. *Journal of Geophysical Research*, *98*(B12), 21,865–21,876. <https://doi.org/10.1029/93JB02391>
- Hyndman, R. D., Yamano, M., & Oleskevich, D. A. (1997). The seismogenic zone of subduction thrust faults. *Island Arc*, *6*(3), 244–260. <https://doi.org/10.1111/j.1440-1738.1997.tb00175.x>
- Illies, J. H. (1981). Mechanism of graben formation. *Tectonophysics*, *73*(1–3), 249–266. [https://doi.org/10.1016/0040-1951\(81\)90186-4](https://doi.org/10.1016/0040-1951(81)90186-4)
- Johnson, H. P., Miller, U. K., Salmi, M. S., & Solomon, E. A. (2015). Analysis of bubble plume distributions to evaluate methane hydrate decomposition on the continental slope. *Geochemistry, Geophysics, Geosystems*, *16*, 3825–3839. <https://doi.org/10.1002/2015GC005955>
- Judd, A. G., & Hovland, M. (1992). The evidence of shallow gas in marine sediments. *Continental Shelf Research*, *12*(10), 1081–1095. [https://doi.org/10.1016/0278-4343\(92\)90070-Z](https://doi.org/10.1016/0278-4343(92)90070-Z)
- Kannberg, P. K., Trehu, A. M., Pierce, S. D., Paull, C. K., & Caress, D. W. (2013). Temporal variation of methane flares in the ocean above Hydrate Ridge, Oregon. *Earth Planet Science Letters*, *368*, 33–42.
- Kastner, M., Solomon, E. A., Harris, R. N., & Torres, M. E. (2014). Fluid origins, thermal regimes, and fluid and solute fluxes in the forearc of subduction zones. *Developments in Marine Geology*, *7*, 671–733. <https://doi.org/10.1016/B978-0-444-62617-2.00022-0>
- Kukowski, N., Greinert, J., & Henrys, S. (2010). Morphometric and critical taper analysis of the Rock Garden region, Hikurangi Margin, New Zealand: Implications for slope stability and potential tsunami generation. *Marine Geology*, *272*(1–4), 141–153. <https://doi.org/10.1016/j.margeo.2009.06.004>
- Lauer, R. M., & Saffer, D. M. (2015). The impact of splay faults on fluid flow, solute transport, and pore pressure distribution in subduction zones: A case study offshore the Nicoya Peninsula, Costa Rica. *Geochemistry, Geophysics, Geosystems*, *16*, 1089–1104. <https://doi.org/10.1002/2014GC005638>
- Li, L., Lei, X., Zhang, X., & Sha, Z. (2013). Gas hydrate and associated free gas in the Dongsha area of northern South China Sea. *Marine and Petroleum Geology*, *39*(1), 92–101. <https://doi.org/10.1016/j.marpetgeo.2012.09.007>
- Lister, G., Tkalčić, H., Hejrani, B., Koulali, A., Rohling, E., Forster, M., & McClusky, S. (2018). Lineaments and earthquake ruptures on the East Japan megathrust. *Lithosphere*, *10*(4), 512–522. <https://doi.org/10.1130/L687.1>
- Loher, M., Marcon, Y., Pape, T., Römer, M., Wintersteller, P., Ferreira, C. S., et al. (2018). Seafloor sealing, doming, and collapse associated with gas seeps and authigenic carbonate structures at Venere mud volcano, Central Mediterranean. *Deep Sea Research Part I: Oceanographic Research Papers*, *137*, 76–96. <https://doi.org/10.1016/j.dsr.2018.04.006>
- Mau, S., Gentz, T., Körber, J. H., Torres, M. E., Römer, M., Sahling, H., et al. (2015). Seasonal methane accumulation and release from a gas emission site in the Central North Sea. *Biogeosciences*, *12*(18), 5261–5276. <https://doi.org/10.5194/bg-12-5261-2015>
- McCaffrey, R. (2009). Time-dependent inversion of three-component continuous GPS for steady and transient sources in northern Cascadia. *Geophysical Research Letters*, *36*, L07304. <https://doi.org/10.1029/2008GL036784>
- McCrory, P. A., Blair, J. L., Waldhauser, F., & Oppenheimer, D. H. (2012). Juan de Fuca slab geometry and its relation to Wadati-Benioff zone seismicity. *Journal of Geophysical Research*, *117*, B09306. <https://doi.org/10.1029/2012JB009407>
- McCrory, P. A., Foster, D. S., Danforth, W. W., Hamer, M. R., & Kayen, R. (2002). *Crustal Deformation at the Leading Edge of the Oregon Coast Range Block, Offshore Washington (Columbia River to Hoh River)*. Washington DC: U.S. Government Printing Office.
- McNeill, C., Piper, A., Goldfinger, C., Kulm, L. D., & Yeats, S. (1998). Listric normal faulting on the Cascadia continental margin coast range. *Journal of Geophysical Research*, *102*(B6), 12,123–12,138. <https://doi.org/10.1029/97JB00728>
- Melnick, D., Moreno, M., Motagh, M., Cisternas, M., & Wesson, R. L. (2012). Splay fault slip during the M_w 8.8 2010 Maule Chile earthquake. *Geology*, *40*(3), 251–254.
- Michael, H. A., Mulligan, A. E., & Harvey, C. F. (2005). Seasonal oscillations in water exchange between aquifers and the coastal ocean. *Nature*, *436*(7054), 1145–1148. <https://doi.org/10.1038/nature03935>
- Moore, J. C., & Saffer, D. (2001). Updip limit of the seismogenic zone beneath the accretionary prism of Southwest Japan: An effect of diagenetic to low-grade metamorphic processes and increasing effective stress. *Geology*, *29*(2), 183–186. [https://doi.org/10.1130/0091-7613\(2001\)029<0183:ULOTSZ>2.0.CO;2](https://doi.org/10.1130/0091-7613(2001)029<0183:ULOTSZ>2.0.CO;2)
- Muller-Karger, F. E., Varela, R., Thunell, R., Luerssen, R., Hu, C., & Walsh, J. J. (2005). The importance of continental margins in the global carbon cycle. *Geophysical Research Letters*, *32*, L01602. <https://doi.org/10.1029/2004GL021346>
- Oleskevich, D. A., Hyndman, R. D., & Wang, K. (1999). The updip and downdip limits to great subduction earthquakes: Thermal and structural models of Cascadia, South Alaska, SW Japan, and Chile. *Journal of Geophysical Research*, *104*(B7), 14,965–14,991. <https://doi.org/10.1029/1999JB900060>

- Olsen, K. B., Stephenson, W. J., & Geisselmeyer, A. (2008). 3D crustal structure and long-period ground motions from a M9.0 megathrust earthquake in the Pacific Northwest region. *Journal of Seismology*, *12*(2), 145–159. <https://doi.org/10.1007/s10950-007-9082-y>
- Orange, D., Greene, H., Reed, D., & Martin, J. (1999). Widespread fluid expulsion on a translational continental margin: Mud volcanoes, fault zones, headless canyons, and organic-rich substrates in Monterey Bay, California. *Geological Society of America Bulletin*, *111*(7), 992–1009. [https://doi.org/10.1130/0016-7606\(1999\)111<0992:WFEOAT>2.3.CO;2](https://doi.org/10.1130/0016-7606(1999)111<0992:WFEOAT>2.3.CO;2)
- Palmer, S. P., & Lingley, W. S. Jr. (1989). *An Assessment of the Oil and Gas Potential of the Washington Outer Continental Shelf: Seattle*. Washington: University of Washington Sea Grant Program.
- Phrampus, B. J., Harris, R. N., & Tréhu, A. M. (2017). Heat flow bounds over the Cascadia margin derived from bottom simulating reflectors and implications for thermal models of subduction. *Geochemistry, Geophysics, Geosystems*, *18*, 3309–3326. <https://doi.org/10.1002/2017GC007077>
- Plafker, G. (1969). Tectonics of the March 27, 1964 Alaska earthquake: U.S. Geological Survey Professional Paper 543–I, 74 p., 2 sheets, scales 1:2,000,000 and 1:500,000. Retrieved from <https://pubs.usgs.gov/pp/0543i/>
- Post, V. E. A., Groen, J., Kooi, H., Person, M., Ge, S., & Edmunds, W. M. (2013). Offshore fresh groundwater reserves as a global phenomenon. *Nature*, *504*(7478), 71–78. <https://doi.org/10.1038/nature12858>
- Puig, P., Durán, R., Muñoz, A., Elvira, E., & Guillén, J. (2017). Submarine canyon-head morphologies and inferred sediment transport processes in the Alías-Almanzora canyon system (SW Mediterranean): On the role of the sediment supply. *Marine Geology*, *393*, 21–34. <https://doi.org/10.1016/j.margeo.2017.02.009>
- Rau, W. W. (1973). *Geology of the Washington Coast between Point Grenville and the Hoh River*. Washington: Department of Natural Resources.
- Rau, W. W., & Grocock, G. R. (1974). *Piercement Structure Outcrops Along the Washington Coast*. Washington (State): Division of Geology and Earth Resources.
- Riedel, M., Scherwath, M., Römer, M., Veloso, M., Heesemann, M., & Spence, G. D. (2018). Distributed natural gas venting offshore along the Cascadia margin. *Nature Communications* *9*, 3264.
- Riedel, M., Spence, G. D., Chapman, N. R., & Hyndman, R. D. (2002). Seismic investigations of a vent field associated with gas hydrates, offshore Vancouver Island. *Journal of Geophysical Research*, *107*(B9), 13308. <https://doi.org/10.1029/2001JB000269>
- Roeloffs, E. A. (1998). Persistent water level changes in a well near Parkfield, California, due to local and distant earthquakes. *Journal of Geophysical Research*, *103*(B1), 869–889. <https://doi.org/10.1029/97JB02335>
- Saffer, D. M., Underwood, M. B., & Mckiernan, A. W. (2008). Evaluation of factors controlling smectite transformation and fluid production in subduction zones: Applications to Nankai Trough. *Island Arc*, *17*(2), 208–230. <https://doi.org/10.1111/j.1440-1738.2008.00614.x>
- Salmi, M. S., Johnson, H. P., & Harris, R. N. (2017). Thermal environment of the Southern Washington region of the Cascadia Subduction Zone. *Journal of Geophysical Research: Solid Earth*, *122*, 5852–5870. <https://doi.org/10.1002/2016JB013839>
- Salmi, M. S., Johnson, H. P., Leifer, I., & Keister, J. E. (2011). Behavior of methane seep bubbles over a pockmark on the Cascadia continental margin. *Geosphere*, *7*(6), 1273–1283. <https://doi.org/10.1130/GES00648.1>
- Sample, J. C., Reid, M. R., Tols, H. J., & Moore, J. C. (1993). Carbonate cements indicate channeled fluid flow along a zone of vertical faults at the deformation front of the Cascadia accretionary wedge (northwest US coast). *Geology*, *21*(6), 507–510. [https://doi.org/10.1130/0091-7613\(1993\)021<0507:CCICFF>2.3.CO;2](https://doi.org/10.1130/0091-7613(1993)021<0507:CCICFF>2.3.CO;2)
- Schliche, R. W. (1991). Half-graben basin filling models: New constraints on continental extensional basin development. *Basin Research*, *3*(3), 123–141. <https://doi.org/10.1111/j.1365-2117.1991.tb00123.x>
- Snively, P. D. Jr. (1987). Tertiary geologic framework, Neotectonics, and petroleum potential of the Oregon-Washington continental margin.
- Snively, P. D. Jr., & Wagner, H. C. (1982). *Geologic Cross Section Across the Continental Margin of Southwestern Washington*. No. 82-459. Reston, Virginia: US Geological Survey.
- Spence, G. D., Minshull, T. A., & Fink, C. (1995). Seismic studies of methane gas hydrate, offshore Vancouver Island. In *Proceedings-Ocean Drilling Program Scientific Results* (pp. 163–174). Alexandria, VA: National Science Foundation.
- Suess, E. (2014). Marine cold seeps and their manifestations: Geological control, biogeochemical criteria and environmental conditions. *International Journal of Earth Sciences*, *103*(7), 1889–1916. <https://doi.org/10.1007/s00531-014-1010-0>
- Thomsen, L., Barnes, C., Best, M., Chapman, R., Pirenne, B., Thomson, R., & Vogt, J. (2012). Ocean circulation promotes methane release from gas hydrate outcrops at the NEPTUNE Canada Barkley canyon node. *Geophysical Research Letters*, *39*, L16605. <https://doi.org/10.1029/2012GL052462>
- Torres, M. E., Embley, R. W., Merle, S. G., Trehu, A. M., Collier, R. W., Suess, E., & Heeschen, K. U. (2009). Methane sources feeding cold seeps on the shelf and upper continental slope off central Oregon, USA. *Geochemistry, Geophysics, Geosystems*, *10*, Q11003. <https://doi.org/10.1029/2009GC002518>
- Torres, M. E., McManus, J., Hammond, D. E., De Angelis, M. A., Heeschen, K. U., Colbert, S. L., et al. (2002). Fluid and chemical fluxes in and out of sediments hosting methane hydrate deposits on hydrate ridge, OR, I: Hydrological provinces. *Earth and Planetary Science Letters*, *201*(3-4), 525–540. [https://doi.org/10.1016/S0012-821X\(02\)00733-1](https://doi.org/10.1016/S0012-821X(02)00733-1)
- Tsuji, T., Ashi, J., Strasser, M., & Kimura, G. (2015). Identification of the static backstop and its influence on the evolution of the accretionary prism in the Nankai Trough. *Earth and Planetary Science Letters*, *431*, 15–25. <https://doi.org/10.1016/j.epsl.2015.09.011>
- Wagner, H. C., & Batatian, L. D. (1986). Preliminary geologic framework studies showing bathymetry, Locations of Geophysical Tracklines and Exploratory Wells, Sea Floor Geology and Deeper Geologic Structures, Magnetic Contours, and Inferred Thickness of Tertiary Rocks on the Continental Shelf and Upper Continental Slope Off Southwestern Washington Between Latitudes 46°N and 47°30'N and from the Washington Coast to 125°20'W. Washington Department of Natural Resources, Division of Geology and Earth Resources.
- Wang, K., & Hu, Y. (2006). Accretionary prisms in subduction earthquake cycles: The theory of dynamic Coulomb wedge. *Journal of Geophysical Research*, *111*, B06410. <https://doi.org/10.1029/2005JB004094>
- Wang, K., Hu, Y., & He, J. (2012). Deformation cycles of subduction earthquakes in a viscoelastic Earth. *Nature*, *484*(7394), 327–332. <https://doi.org/10.1038/nature11032>
- Wang, K., Hyndman, R. D., & Davis, E. E. (1993). Thermal effects of sediment thickening and fluid expulsion in accretionary prisms: Model and parameter analysis. *Journal of Geophysical Research*, *98*(B6), 9975–9984. <https://doi.org/10.1029/93JB00506>
- Wang, K., & Tréhu, A. M. (2016). Invited review paper: Some outstanding issues in the study of great megathrust earthquakes—The Cascadia example. *Journal of Geodynamics*, *98*, 1–18. <https://doi.org/10.1016/j.jog.2016.03.010>
- Wang, K., Wells, R., Mazzotti, S., Hyndman, R. D., & Sagiya, T. (2003). A revised dislocation model of interseismic deformation of the Cascadia subduction zone. *Journal of Geophysical Research*, *108*(B1), 2026. <https://doi.org/10.1029/2001JB001227>

- Wang, P.-L., Engelhart, S. E., Wang, K., Hawkes, A. D., Horton, B. P., Nelson, A. R., & Witter, R. C. (2013). Heterogeneous rupture in the great Cascadia earthquake of 1700 inferred from coastal subsidence estimates. *Journal of Geophysical Research: Solid Earth*, *118*, 2460–2473. <https://doi.org/10.1002/jgrb.50101>
- Weinstein, A., Navarrete, L., Ruppel, C., Weber, T. C., Leonte, M., Kellermann, M. Y., et al. (2016). Determining the flux of methane into Hudson Canyon at the edge of methane clathrate hydrate stability. *Geochemistry, Geophysics, Geosystems*, *17*, 3882–3892. <https://doi.org/10.1002/2016GC006421>
- Yuan, T., Hyndman, R. D., Spence, G. D., & Desmons, B. (1996). Seismic velocity increase and deep-sea gas hydrate concentration above a bottom-simulating reflector on the northern Cascadia continental slope. *Journal of Geophysical Research*, *101*(B6), 13,655–13,671. <https://doi.org/10.1029/96JB00102>
- Yuan, T., Spence, G. D., & Hyndman, R. D. (1994). Seismic velocities and inferred porosities in the accretionary wedge sediments at the Cascadia margin. *Journal of Geophysical Research*, *99*(B3), 4413–4427. <https://doi.org/10.1029/93JB03203>